A Comparison between α and Proton Sequential Emission in the $^{16}O(133\ \mathrm{MeV}) + {}^{58}Ni$ Deep Inelastic Collision

R. Barná, D. De Pasquale, A. Italiano, A. Trifiró, M. Trimarchi
Istituto Nazionale di Fisica Nucleare, Gruppo Collegato di Messina - Messina
Dipartimento di Fisica dell'Università - Messina
Salita Sperone 31, Vill. S. Agata 98166 Messina, Italy

A. Strazzeri
Dipartimento di Fisica dell'Università - Catania
Istituto Nazionale di Fisica Nucleare, Sezione di Catania - Catania
Corso Italia 57, 95129 Catania, Italy

V. Rauch, C. Beck, T. Bellot, C. Bhattacharya*, D. Disdier†, R.M. Freeman, F. Haas, R. Nouicer‡, P. Papka, M. Rousseau§, and O. Stezowski¶
Institut de Recherches Subatomiques, UMR7500,
IN2P3/CNRS - Université Louis Pasteur Strasbourg,
23, rue du Loess, B.P. 28, F-67037 Strasbourg Cedex 2, France

March 15, 2002

Abstract

The deep-inelastic processes of the ^{16}O + ^{58}Ni reaction have been investigated by using coincident charged particle tecniques. Inclusive as well as exclusive data of the C, N, and O fully-damped fragments and their associated light charged particles (p, d, t, and α-particles) were collected at the IReS Strasbourg VIVITRON Tandem facility at the $E_{lab}(^{16}\mathrm{O}) = 133$ MeV bombarding energy by using the ICARE charged particle multidetector array, which consists of 48 telescopes. The measured energy spectra, velocity distributions, and in-plane angular correlations are analysed by a semiclassical model describing both the nonequilibrium and the evaporative components of a deep-inelastic reaction mechanism in a single picture. This closed-form theoretical approach is applied, in the hypothesis of a sequential process, to the $((C,N,O)-p)$ and $(C,N,O)-\alpha)$ differential multiplicities for the $^{16}O + {}^{58}Ni$ at 8.3 MeV/nucleon deep-inelastic collision. From this analysis some reaction mechanism information, such as on polarization phenomena and on "decay times" estimates, can be deduced.

PACS number(s): 25.70.Gh, 25.70.Jj, 25.70.Mn, 24.60.Dr

*Permanent address: VECC, 1/AF Bidhan Nagar, Kolkata 64, India.
†Deceased
‡Present address: Department of Physics, University of Illinois at Chicago, Chicago, Illinois 60607-7059, USA.
§Present address: University of Surrey, Guildford GU2 7XH, United Kingdom.
¶Permanent address: IPN Lyon, F-69622 Villeurbanne, France.

1 INTRODUCTION

The study of dinuclear systems formed in peripheral heavy-ion reactions as well as in deep-inelastic (DI) collisions at low bombarding energies not exceeding 10 MeV/nucleon [1] is still an interesting domain of research since the subsequent decay of these dinuclear objects by light-particle sequential emission is still not well understood. The light particle emission in DI collisions is a very powerful tool to investigate the various mechanims leading to the strong energy dissipation typical of this kind of reaction mechanisms [2, 3, 4, 5, 6, 7, 8, 9, 10]. DI collisions involve a large transfer of angular momentum from the entrance channel to the intrinsic spins of the outgoing fragments. The amount of the momentum transferred, and its alignment, can be studied by measuring the angular distributions of the decay products of the excited target-like fragments (TLF) with respect to their recoil directions. Several studies of sequential processes [2, 4, 6, 7] have revealed that the measured in-plane angular correlations are sharply forward-peaked, and not symmetric with respect either to the direction of the coincident projectile-like fragment (PLF), or to the beam axis, with marked differences between distributions for positive and negative angles [6, 7]. Then and despite of the known sequential decay modes of DI fragments, clear experimental evidences were found for the occurence of an additional fast nonequilibrium emission of α particles in the ^{16}O + ^{58}Ni reaction between 6 and 9 MeV/nucleon [4, 6]. This fast α-decay mode implies that the reaction time has to be small compared to the rotational period of the intermediate dinuclear system. In order to describe this experimental behaviour we have developed in a recent publication [11] a semiclassical approach [12, 13, 14], which accomodates both the fast nonequilibrium components and the slower evaporative contributions (equilibrium components) of the sequential particle emission in peripheral heavy-ion collisions in a simple way. This approach [14] was first applied [11] to measured angular correlations between α particles and PLF's arising from the $^{16}O(96\ \mathrm{MeV}) + {}^{58}Ni$ [4, 6] and $^{16}O(133\ \mathrm{MeV}) + {}^{48}Ti$ [11] DI collisions. Here we report on the analysis of the α and proton pre-equilibrium emission in the ^{16}O + ^{58}Ni reaction. To this aim a new measurement on this reaction at E_{lab} = 133 MeV has been performed at the VIVITRON Tandem facility with the ICARE charged particle multidetector array [15, 16, 17]. The anglar correlations of protons have been measured for the first time for the $^{16}O + {}^{58}Ni$ reaction. A comparison between the two kinds of emission (nonequilibrium and evaporative components) for both α particles and protons is proposed to give further information on the reaction mechanism: for example polarization effects and estimates of "decay times".

The paper is organized in the following way. After a short description of the experimental techniques, the experimental results are presented in Section II (part of the work presented here in detail have already been briefly reported elsewhere [18]). In Section III reference to theoretical background is first given before a general discussion of the the present $^{16}O + {}^{58}Ni$ experimental data. The semiclassical approach to particle - particle angular correlations is applied, and a comparison between $(C, N, O) - \alpha$ and $(C, N, O) - p$ angular correlations is carried out. Concluding remarks are finally proposed in Section IV, after a brief summary.

2 EXPERIMENTAL TECHNIQUES AND RESULTS

In the present experiment, the α particles associated with the (C, N, O) fragments are emitted by (Zn, Cu, Ni) intermediate nuclei during the sequential reaction

$$\begin{aligned} {}^{16}O + {}^{58}Ni &\rightarrow (C,N,O) + (Zn^*, Cu^*, Ni^*) + Q_2 \\ &\rightarrow (C,N,O) + (Ni, Co, Fe) + \alpha + Q_3; \end{aligned} \quad (1)$$

similarly, the protons associated with the (C, N, O) fragments are emitted by (Zn, Cu, Ni) intermediate nuclei during the sequential reaction

$$\begin{aligned} {}^{16}O + {}^{58}Ni &\rightarrow (C,N,O) + (Zn^*, Cu^*, Ni^*) + Q_2 \\ &\rightarrow (C,N,O) + (Cu, Ni, Co) + p + Q_3. \end{aligned} \quad (2)$$

2.1 Experimental setup

The experiment was performed at the IReS Strasbourg VIVITRON Tandem facility using a 133 MeV ^{16}O beam which was incident on an isotopically enriched ^{58}Ni (750 $\mu g/cm^2$ thick) target mounted in the ICARE scattering chamber [15, 16, 17]. The main purpose of this work is to investigate the *in-plane* angular correlations between C, N, O PLF's and light particles (α,p). Therefore, as an application of the theoretical approach that has been recently proposed by Barna *et al.* [11], and which will be presented in the next Section, we have measured the $((C,N,O)-\alpha)$ and $((C,N,O)-p)$ differential multiplicities, respectively, arising from the ^{16}O(133 MeV) + ^{58}Ni DI collision.

Both the heavy ions (A $\geq$ 6) and their associated LCP's (p, d, t, and α particles) were detected using the ICARE charged particle multidetector array [15, 16, 17] which consists of 48 telescopes in coincidence. The strongly energy-damped PLF's (C,N,O)-ions were detected in 10 gas-silicon hybrid telescopes (IC), each composed of a 4.8 cm thick ionization chamber, with a thin Mylar entrance window, followed by a 500 μm thick Si(SB) detector. The IC telescopes allow a good resolution in emission angle, kinetic energy, and Z of the detected particle. To lower the detection threshold for light charged particles (LCP) their time-of-flight were measured in addition to provide a mass identification. Three of the IC's were placed at an angle of $\vartheta_{lab} = 30°$ with respect to the beam direction, well above the grazing angle ($\vartheta_{grazing} = 20°$ for the studied system). Fig. 1.a) displays a typical example of charge identification which can be achieved from the E-ΔE two-dimensional spectrum registered for the ^{16}O + ^{58}Ni reaction E$_{lab}$ = 133 MeV at $\vartheta_{lab} = 30°$. This plot shows how clearly the identification of the fragments can be achieved, due to the excellent charge resolution by the IC's allowing us to distinguish among them.

2.2 Experimental procedures and data analysis

Since we are interested in the investigation of the angular correlations mainly in the reaction plane, 33 telescopes (of the total number of 48 telescopes) of ICARE have located in the reaction chamber on two rings intersecting each other along the beam direction. Two IC telescopes were mounted on the first ring, at $\vartheta_{lab} = +30°$ and $\vartheta_{lab} = -30°$ with respect to the beam axis, while a third one was mounted on the second ring, at $\vartheta_{lab} = +30°$. 7 IC telescopes were mounted (on the first ring) at backward angles ($\vartheta \geq 120°$), having a low-energy threshold needed to detect very low energy

particles emitted in the backward angle region. The IC's were filled with isobutane at a pressure of 120 Torr for the backward angle telescopes and of 60 Torr for the forward angle detectors, thus allowing for the simultaneous measurement of both light and heavy fragments. The acceptance of each telescope was defined by thick aluminium collimators.

The in-plane detection of coincident LCP's was done using 16 two-element telescopes (40 μm Si, 2 cm CsI(Tl)), with high-energy thresholds, mounted - on the first ring - in the $\vartheta_{lab} = 40^\circ \div 120^\circ$ angular range, and 7 three-element telescopes (40 μm Si, 300 μm Si, and 2 cm CsI(Tl)) mounted on both rings, between $\vartheta_{lab} = 10^\circ$ and $\vartheta_{lab} = 35^\circ$, angular range where the kinetic energy of the light particles peaks at his maximum. By adopting this geometry, collection of the coincidences between the PLF telescopes and each LCP telescope for both rings allowed the investigation of 54 angles on the whole in-plane angular angle. The CsI(Tl) scintillators were coupled to photodiode readouts. Fig. 1.b) displays a bidimensional E-δE spectrum, which refers to the lighter fragments (lower spectrum) and was registered for the ^{16}O + ^{58}Ni reaction E_{lab} = 133 MeV at $\vartheta_{lab} = 30^\circ$. The charge and mass identifications for p, d, and t as well as for ^{3}He and α particles have been clearly achieved for all LCP telescopes.

The energy calibrations of the different telescopes of the ICARE multidetector array were carried out using ^{228}Th and ^{241}Am radioactive α-particle sources in the 5-9 MeV energy range, a precision pulser, and elastic scatterings of 133 MeV ^{16}O from ^{197}Au, ^{58}Ni, and ^{12}C targets in a standard manner. In addition, the ^{12}C(^{16}O,α)^{24}Mg* reaction at E_{lab} = 53 MeV [17] was used to provide known energies of α particles feeding the ^{24}Mg excited states, thus allowing for calibration of the backward angle detectors. The proton calibration was carried out using scattered protons from formvar targets bombarded in reversed kinematics reactions with the two ^{16}O beams. More details on the experimental setup of ICARE and on the experimental procedures can be found in Refs. [17, 19, 20].

2.3 Experimental results

The velocity contour maps of the LCP Galilean invariant differential cross-sections $(d^2\sigma/d\Omega dE)p^{-1}c^{-1}$ as a function of the LCP velocity provides an overall picture of the reaction pattern. Fig. 2 shows such a plot of invariant cross-section in the ($V_{||}$,$V_\perp$) plane for α particles measured in coincidence with C, N and O fragments emitted at 30°. The symbols $V_{||}$ and $V_\perp$ denote laboratory velocity components parallel and perpendicular to the beam, respectively. Fig. 3 shows the analogous velocity plots for protons when fragments are detected at $\Theta_{lab} = 30^\circ$.

In Fig. 2 and Fig. 3 the arrows correspond to the recoil velocities of the TLF and PLF emission sources, respectively. The radii of the circles associated with the TLF emission sources have been calculated by assuming the respective Coulomb barriers of α-TLF and p-TLF. The ellipsoidal curves drawn in Fig. 2 are centered on the PLF velocities, and have been calculated by fixing the PLF excitation energies to their most probable values : i.e. 10 MeV, 6 MeV, and 7 MeV for O*, F*, and Ne* fragments, respectively [16]. These curves display the occurence of the two different kinematical solutions which are also visible in the experimental data. The comparison of the velocity diagrams for the ^{58}Ni and ^{12}C targets allow to distinguish a third α component due to the C build-up contamination of the ^{58}Ni target. The amount of carbon impurity in the ^{58}Ni target was estimated to be of approximately 10 μg/cm^2. This component

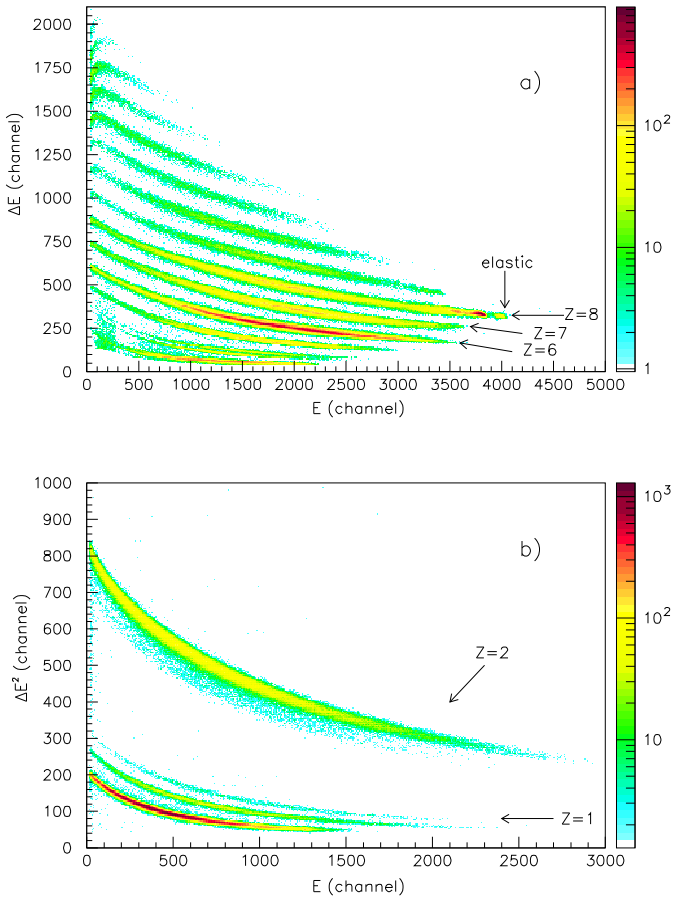

Figure 1: *Examples of charge identification from two typical E-ΔE bidimensional spectra for the $^{16}O + {}^{58}Ni$ reaction at $E_{lab} = 133$ MeV.*

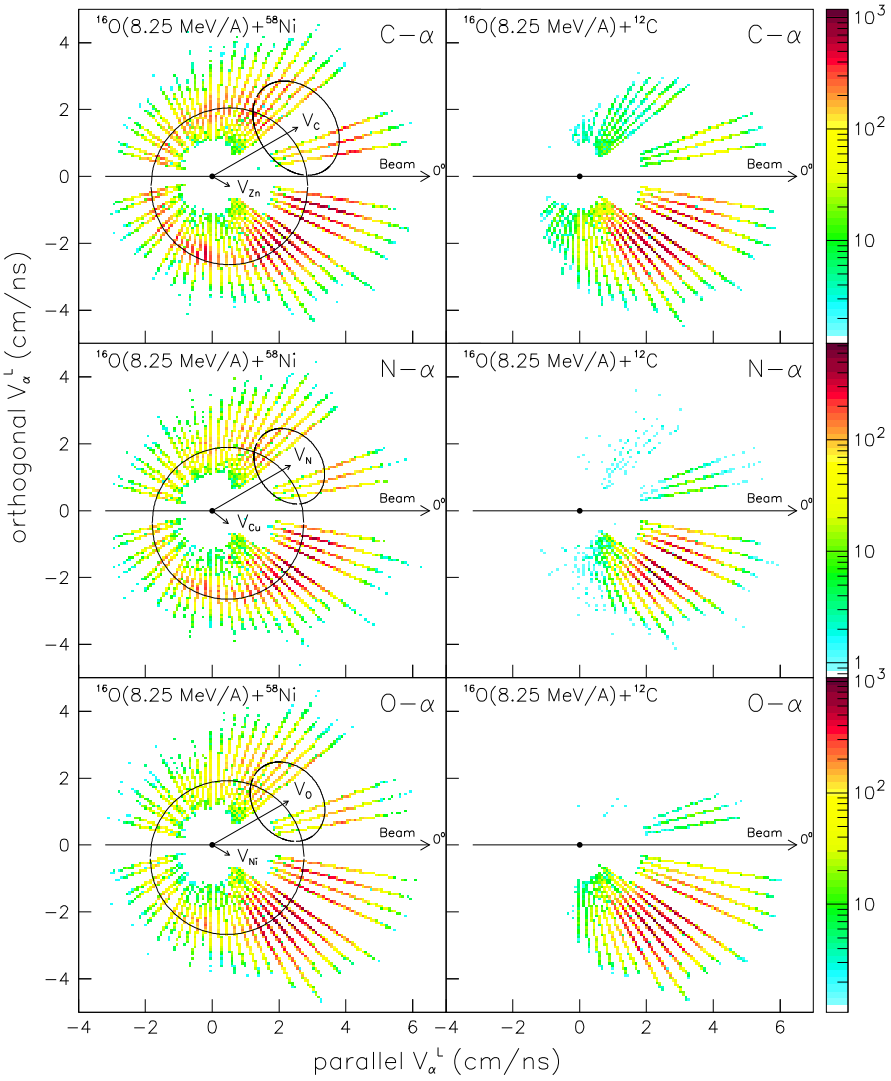

Figure 2: *Exclusive Galilean invariant cross-section* $(d^2\sigma/d\Omega dE)p^{-1}c^{-1}$ *of* α *particles in coincidence with* C, N, O *fragments identified in a IC located at* $\Theta^C_{lab} = 30^o$*, as plotted in the* $(V_{\|}, V_{\perp})$ *plane for the* $^{16}O + ^{58}Ni$ *(left side) and* $^{16}O + ^{12}C$ *(right side) reactions at* $E_{lab} = 133$ *MeV.*

is essentially present in the forward-angle region. To extract the equilibrium and non-equilibrium sequential components, all different processes contributing to the α- and p-emission, *e.g.* the α particles arising from the C build-up contamination and the break-up events, were identified and removed following the procedure described in detail in Ref. [16].

The analyzed in-plane angular correlations have been referred to the Recoil Centre of Mass System (*i.e.* to the C.M. systems of Zn, Cu and Ni, respectively.

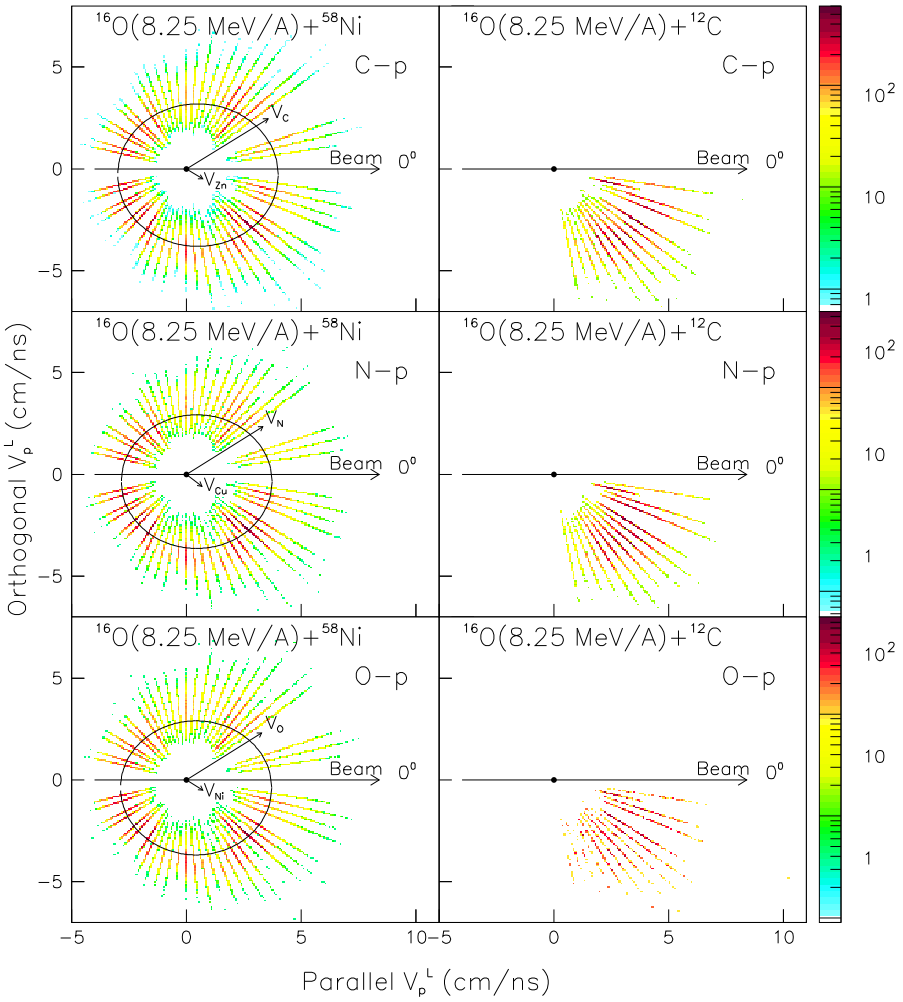

Figure 3: *Exclusive Galilean invariant cross-section* $(d^2\sigma/d\Omega dE)p^{-1}c^{-1}$ *of protons in coincidence with* C, N, O *fragments identified in a IC located at* $\Theta^C_{lab} = 30°$*, as plotted in the* $(V_{||}, V_\perp)$ *plane for the* $^{16}O + ^{58}Ni$ *and* $^{16}O + ^{12}C$ *reactions at* $E_{lab} = 133$ *MeV.*

Fig. 4 shows the experimental data of the cross-sections for $(C-\alpha)$, $(N-\alpha)$ and $(O-\alpha)$ coincidences together with the theoretical curves described in the following Section, plotted vs. the in-plane α-angle measured with respect to the beam direction, respectively. The forward-angle region appears to be dominated by the preequilibrium component, which strongly depends on the mechanism of the first reaction step, while at backward angles only the equilibrium emission is present, and this component is

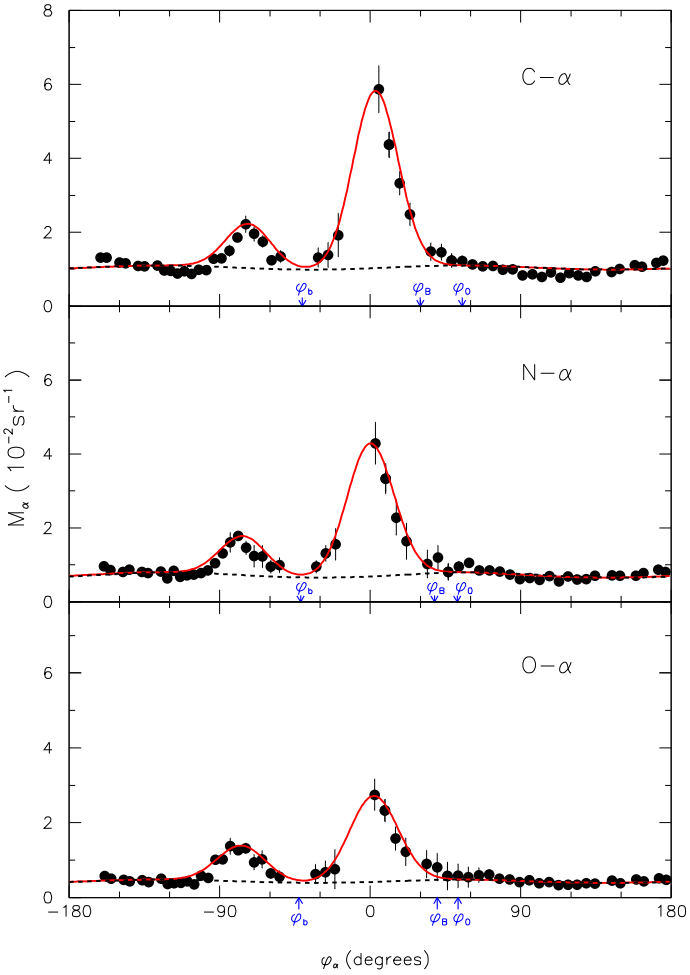

Figure 4: *Best-fit of the in-plane $C-\alpha$, $N-\alpha$ and $O-\alpha$ differential multiplicity data, for the $^{16}O+^{58}Ni$ reaction at E_{lab} = 133 MeV. The differential multiplicities, in $10^{-2}sr^{-1}$ units, are plotted vs. the in-plane α-angle. The arrows indicate the directions of the PLF (b) and TLF (B) with respect to the incident beam in the laboratory system. The solid curves represent the total multiplicities, while the dashed curves represent the equilibrium component.*

almost isotropic for all the three coincident exit-channels. Fig. 5 reports the in-plane differential multiplicities of $(C-p)$, $(N-p)$ and $(O-p)$ vs. the φ_p angle. The same y-scale adopted in both figures 4 and 5 allows a direct comparison of the differential multiplicities for the α and proton emissions, respectively.

3 SEMICLASSICAL APPROACH TO PARTICLE-PARTICLE ANGULAR CORRELATION

3.1 Theoretical background

Let us recall some fundamental formulas for a better understanding of the physical meaning of some deduced quantities which will be discussed later in the following Section as well as in the conclusions which will be drawn at the end of the paper. All the theoretical background is described in more detail in Refs. [14, 11].

The main aim of the theoretical approach is to outline a closed-form expression for the b–c multiplicity of a sequential process like $A(a,b)B(c)C$ showing that an important and remarkable nonequilibrium component in the particle emission is present even in the case of a sequential process. We also show how useful conclusions on the mechanism of a peripheral collision $A(a,b)B$ can be drawn from the investigation of the b–c angular correlation pattern around the forward angles.

Following closely the definitions and approximations of Ref. [14], we start by considering a sequential process like $A(a,b)B(c)C$ and we assume it proceeds through a given continuum state $(\epsilon^\star_B, J_B\pi_B)$ in the nucleus B to a narrow definite state $(\epsilon^\star_C, J_C\pi_C)$ in the final nucleus C.

In the following, $\epsilon^\star_X$ indicates the excitation energy of the state of definite spin J_X and parity π_X in the nucleus X and m_X the z-component of $\vec{J}_X$. The pair (xX) has relative radial coordinate $\vec{r}_x$, momentum $\vec{k}_x$, velocity $\vec{v}_x$ and energy ϵ_x. The spherical polar angles (ϑ_b, φ_b) of $\vec{k}_b$ are defined in the $(A+a)$ centre-of-mass (c.m.) system, while $\vec{k}_c$ has polar angles (ϑ, φ) defined in the recoil centre-of-mass (r.c.m.) system (rest frame of the nucleus B) and described in a xyz-frame with the x-axis and z-axis parallel to the x-axis and z-axis of the c.m. frame.

In order for the $A(a,b)B(c)C$ reaction to be a sequential process, we require that the $\epsilon^\star_B$ excitation energy of the intermediate system B formed in the first step of the three-body reaction be independent of the particle c emission angle and assume, moreover, that in the $B \to c + C$ decay the nuclear interaction between b and B can be neglected; for simplicity, we suppose that the nuclei A, a, b and c have spin zero and b and c are in the ground state.

The average value of the b–c angular correlation over the Δ interval centered at $\epsilon^\star_B$, can be obtained by splitting the $\mathcal{S}$ matrix into an equilibrium (E) and a nonequilibrium (NE) term like [21]

$$\mathcal{S} = \mathcal{S}^E + \mathcal{S}^{NE} \qquad (1a)$$

with

$$\mathcal{S}^E = \mathcal{S} - \langle \mathcal{S} \rangle \qquad (1b)$$

$$\mathcal{S}^{NE} = \langle \mathcal{S} \rangle. \qquad (1c)$$

Moreover we suppose the phase of $\mathcal{S}^E$ and $\mathcal{S}^{NE}$ to be uncorrelated (so that their cross terms average out to zero) and we make the statistical assumption that in the energy

interval Δ around $\epsilon_B^\star$ there are many levels contributing to the $B \to c + C$ decay and that their widths and energies are randomly distributed, so that interference terms generally vanish [22, 23].

We also assume that the amplitude $\mathcal{S}^{NE}$ (see eq.(1c)) is a very smoothly varying function of the excitation energy $\epsilon_C^\star$ within a $\Delta'(\sim \Delta)$ region.

Following restrictions and approximations of Ref. [14], we can express the energy averaged $b-c$ angular correlation as the sum

$$\langle \frac{d^2\sigma}{d\omega_b d\omega} \rangle = \left(\frac{d^2\sigma}{d\omega_b d\omega} \right)^E + \left(\frac{d^2\sigma}{d\omega_b d\omega} \right)^{NE} \tag{2}$$

with

$$\left(\frac{d^2\sigma}{d\omega_b d\omega} \right)^E = \sum_{m_C} \sum_{\ell J_C} w_\ell(J_C) (\frac{T_\ell}{G}) \mid \sum_{m_B} p_\ell(m_B, m_C; \omega_b, \omega) \mid^2 \tag{3}$$

$$\left(\frac{d^2\sigma}{d\omega_b d\omega} \right)^{NE} = \sum_{m_C} \mid \sum_{\ell J_C} \langle \mathcal{S}_\ell \rangle \sum_{m_B} p_\ell(m_B, m_C; \omega_b, \omega) \mid^2 \tag{4}$$

where

$$p_\ell(m_B, m_C; \omega_b, \omega) \equiv (-)^\ell F_{ba}(m_B, \omega_b) \cdot \\ \cdot \langle \ell J_C, m_B - m_C, m_C \mid J_B m_B \rangle Y_\ell^{m_B - m_C}(\omega). \tag{5}$$

These expressions keep into account the probability of orbital angular momentum ℓ transferred into the $(B; J_B \epsilon_B^\star) \to (cC; \ell J_C \epsilon_C^\star)$ decay and assume the parametrization $\langle \mid \mathcal{S}^E \mid^2 \rangle = T_\ell / G$, where T_ℓ is the optical-model transmission coefficient, G representing all decay energy-allowed modes for the $B \to c + C$ decay [22, 23]. In particular, we are interested in the study of the following kinds of reaction:

$$a + A \to b + B \to b + \alpha + C$$

or

$$a + A \to b + B \to b + p + C$$

The time-dependent scattering theory [24] allows us to assume that the quantity $(d^2\sigma)^{NE}$ can be associated with a situation in which the dissociation of B into c and C is a fast process occurring in time scales by many orders of magnitude shorter than the typical time corresponding to the equilibrium decay process, described by $(d^2\sigma)^E$, whose long lifetime in some way produces a "loss of memory" of the formation of the B decaying nucleus [23]. This is why the angular symmetry of the c-emission from a statistical equilibrated system described by the $b-c$ angular correlation (3) cannot be used as evidence for any particular model of dynamical effect.

The memory of the first step of the sequential process $A(a,b)B(c)C$ can instead be retained during the subsequent "fast" $B \to c+C$ decay, so that the angular dependence of the c particles emerging from such a short-lived composite system can display a marked forward-backward asymmetry around the direction of the coincident projectile residue b or the beam axis. The study of the nonequilibrium sequential component of the particle emission therefore becomes a powerful tool to probe the early stage of the peripheral collision besides a useful alternative technique to obtain reaction mechanism information complementary to what is usually extracted by means of the angular distributions of the two-body reaction products.

Since the angular correlation method is mainly devoted to obtain information on the mechanism of the $A(a,b)B$ reaction and on the polarization effects of the B nucleus , a proper choice would be to adopt coordinate axes such that the z-axis is along $\vec{k}_b \times \vec{k}_a$ (perpendicular to the reaction plane) and the x-axis along $\vec{k}_a$.

Information on the polarization effects of the residual nucleus B induced by the first step of the sequential process $A(a,b)B(c)C$ can also be obtained through the φ-dependence of the differential multiplicity for the second step [14] .

A semiclassical expression for the $b-c$ differential multiplicity has been treated and developed in Ref. [14] which accounts for many of the observed features of the sequential emission of the high as well as low energy particles from the fragments excited in a peripheral heavy-ion reaction

Without going into the details of the theoretical approach, already extensively described and justified in Ref. [14], we consider a semiclassical picture that assumes a coordinate rotation by means of the Euler angles to a more useful system chosen in describing the $B \rightarrow c + C$ decay, where the new quantization axis is oriented in the direction of $\vec{J}_B$ which is at a certain angle Λ with respect to the z-axis and lies in a plane perpendicular to the reaction plane and to the direction of a unit vector $\hat{k}_0$, close to the recoil direction of the decaying nucleus B [25], corresponding to an angle $\varphi_0 = (\pi/2 + \xi)$ with respect to the x-axis; consequently, the relative momentum $\vec{k}_c$ of the pair (cC) has polar angles (ϑ, φ) and (Θ, Φ) with respect to the space-fixed system and to the $(\hat{k}_0 \times \hat{J}_B, \hat{k}_0, \hat{J}_B)$-axes, respectively.

Following the quantal treatment carried out in ref. [26], we assume the semiclassical replacement [26, 27]

$$w_\ell(\mu) \sim \exp(-\alpha \ell^2) \exp(\beta \mu) \tag{7}$$

where

$$\alpha \equiv (\mathcal{I} + MR^2)\hbar^2 / 2\mathcal{I}T_C MR^2$$

$$\beta \equiv J_B \hbar^2 / \mathcal{I}T_C$$

with M, R and $\mathcal{I}$ the reduced mass, the radius and the rigid-body moment of inertia of the pair (cC), respectively, and T_C the nuclear temperature corresponding to the excitation energy $\epsilon_C^\star$ in the C nucleus.

By using the *sharp cut-off* approximation for the coefficient T_ℓ and converting the summation over ℓ to an integral, one obtains

$$(M(\vartheta, \varphi, \Lambda))^E = C_E \exp(-\gamma cos^2 \Theta) \tag{8}$$

C_E being independent of ϑ and φ, while $\gamma \equiv \beta^2/4\alpha$ is the anisotropy coefficient.

The "direct" sequential $B \rightarrow c + C$ decay described by $\langle \mathcal{S} \rangle$ (see eqs. (1)) is naturally attributed to a *prompt* emission of particles from peripheral regions of the nucleus B bearing in mind that in the classical limit the c particles while escaping from the rotating nucleus B gain additional velocity if emitted along the equatorial plane.

We estimate the NE $b-c$ multiplicity by assuming the emission of particles c in the equatorial plane with orbital angular momentum $\vec{\ell}$ parallel to $\vec{J}_B$ to dominate and, consequently, that the peripheral nature of the NE decay process is consistent with the hypothesis that only an "ℓ-window" centered at a certain ℓ_0 contributes. In the amplitude-phase representation, therefore, the energy-averaged element $\langle \mathcal{S}_\ell \rangle$ becomes

$$\langle \mathcal{S}_\ell \rangle = \eta(\ell) \exp[i\delta(\ell)];$$

Moreover, near $\ell = \ell_0$

$$\langle \mathcal{S}_\ell \rangle \sim \eta(\ell - \ell_0) \exp[i(\ell - \ell_0)\chi_0], \tag{9}$$

assuming the $\delta(\ell)$ phase linear in ℓ about ℓ_0 and introducing the *quantal deflection function*:

$$\chi_0 \equiv (\frac{\partial \delta(\ell)}{\partial \ell})_{\ell_0}. \tag{10}$$

The NE differential multiplicity can be written as follows:

$$(M(\vartheta, \varphi, \Lambda))^{NE} \sim \mid Q^{(+)}(\Phi) \mid^2 + h_0 \mid Q^{(-)}(\Phi) \mid^2, \tag{11}$$

where we have defined the "single source" amplitudes

$$Q^{(\pm)}(\Phi) \equiv \sum_\ell \eta(\ell - \ell_0) \exp[i(\ell - \ell_0)(\chi_0 \pm \Phi)].$$

In the approximations and restrictions of Ref. [14], Eq. (11) finally becomes

$$(M(\vartheta, \varphi, \Lambda))^{NE} = C_{NE}\{\exp[-\lambda^2(\Phi + \chi_0)^2] + h_0 \exp[-\lambda^2(\Phi - \chi_0)^2]\} \tag{12}$$

(C_{NE} englobing all the non-essential constants independent of ϑ and φ).
Then, by assuming that the spin orientation is governed by a Gaussian distribution function $L(\Lambda)$ around Λ_0, we have

$$M(\vartheta, \varphi) = \left[(M(\vartheta, \varphi))^E + (M(\vartheta, \varphi))^{NE}\right] \tag{13}$$

with

$$M(\vartheta, \varphi)^E = \int d\Lambda L(\Lambda)(M(\vartheta, \varphi, \Lambda))^E \Big/ \int d\Lambda L(\Lambda) \tag{14}$$

$$M(\vartheta, \varphi)^{NE} = \int d\Lambda L(\Lambda)(M(\vartheta, \varphi, \Lambda))^{NE} \Big/ \int d\Lambda L(\Lambda) \tag{15}$$

where M^E and M^{NE} are given by eqs. (8), (9).

The in-plane differential multiplicity corresponds to $\vartheta = \pi/2$. Moreover when, as in our case, the dealignment is sufficiently small ($\Lambda << 1$), the NE in-plane $b-c$ differential multiplicity is essentially given by a two component asymmetric (in general $h_0 \neq 1$) pattern about the $\xi = \varphi_0 - \pi/2$ angle (see Fig. 2 of Ref. [14]), peaked at the $\varphi_1 = \xi - \chi_0$ and $\varphi_2 = \xi + \chi_0$ angles, respectively; moreover, if $\chi_0 < \xi$ and $h_0 < 1$, the $b-c$ coincidence events most probably appear on the same side of the beam axis with respect to the direction of the "detected" projectile residue. The in-plane coincidence cross-section values around φ_1 and φ_2 correspond to the $A(a,b)B$ reaction process with opposite polarization of B, which may qualitatively be explained by assuming that only one type of "semiclassical trajectory" mainly contributes to the in-plane $b-c$ angular correlation for either positive or negative angles with respect to the direction of the PLF b [28, 30].

In the cases when $\Lambda << 1$, one can obtain an estimate of the ξ angle and of the quantal deflection χ_0 by a simple inspection of the experimental in-plane angular correlation pattern around the "peak angles" φ_1 and φ_2, using the expressions

$$2\xi \simeq \varphi_2 + \varphi_1 \tag{16}$$

$$2\chi_0 \simeq \varphi_2 - \varphi_1. \tag{17}$$

Indeed here the deviation from left-right symmetry in a direction close to the one of the coincident projectile residue as well as the double forward-peaked shape in the angular correlation pattern does not necessarily imply that the light particles emerge from the contact zone between the two colliding nuclei (spatial-localization). Actually, in a simple optical picture, we can interpret the sums appearing in eq. (12) (see also eq. (13)) as a beam of particles c emitted from a "ℓ-window" centered about a mean value ℓ_0 and extended over a narrow width $\Delta\ell \sim \lambda$ (ℓ-localization).

From the above rough picture we somehow idealize the time dependence of the NE $B \rightarrow c + C$ decay; for example the observed strongly forward-peaked in-plane angular correlation can be seen as a signature of an emission of the c light particles in decay times shorter than the B nucleus rotational period, believed to be the time required for a hypothetical complete revolution of the $(c + C)$ composite system.

Moreover, as already shown, a simple, classical picture allows us to link the χ_0 deflection angle to the τ_0 NE decay time, via the rotational frequency $\omega_0 = \hbar\ell_0/\mathcal{I}$:

$$-\chi_0 = \omega_0\tau_0 = \frac{\hbar\ell_0}{\mathcal{I}}\tau_0. \tag{18}$$

3.2 Theoretical analysis

Different multiplicity data plotted in Figs. 4 and 5 for α particles and protons, respectively, have been fitted (solid lines) by the semiclassical equations given before. The dashed and solid lines correspond to the equilibrium and total components, respectively.

Since the mean excitation energy of the emitting TLF is about 60 MeV, a value lying in the continuum region of the excitation spectrum, we can apply the above described theoretical approach to our nuclear system.

For both kinds of spectra, C_E, γ, Λ and Ω parameters were fitted by the purely evaporative formula (13) using the *backward* region data ($\mid \varphi_{light-particle} \mid \geq 100°$), where the experimental data arise primarily from the equilibrium component, and the nonequilibrium term is not present. γ and Λ_0 are not uniquely determined by this procedure, since a range of possibilities can likewise hold; ξ could also be deduced by the evaporative component, but this one is not so sensitive to its choice.

3.2.1 α emission in the ^{16}O + ^{56}Ni reaction

In the case of α emission shown in Fig. 4, the values obtained for the average angle between the spin direction and the normal axis Λ_0 (6° for all the three coincidences) and for the the spin fluctuations Ω (13°) show that the polarization direction of the emitting nucleus is nearly orthogonal to the reaction plane. The fact that the TLF rotational axis lies very close to the z-axis allows an estimate of χ_0 values by rewriting formulas (16,17) as follows:

$$\varphi_1 = \xi - \chi_0 = \varphi_0 - \frac{\pi}{2} - \chi_0 \tag{19}$$

$$\varphi_2 = \xi + \chi_0 = \varphi_0 - \frac{\pi}{2} + \chi_0 \tag{20}$$

Correspondingly, C_{NE}, λ and h_0 parameters were obtained by fitting the *forward* angular region ($\mid \varphi_{light-particle} \mid < 100°$) by means of the (complete) formula (13), after inserting the values of the above-determined C_{NE}, γ, Λ_0, Ω, ξ, χ_0 parameters.

Table 1: **List of the parameters obtained in the analysis of the in-plane PLF-α angular correlations arising from the ^{16}O(133 MeV) + ^{58}Ni reaction.**

Coincidences $(10^{-2} sr^{-1})$	$C_E^{(a)}$	$\gamma^{(a)}$	$\Lambda_0^{(a)}$	$\Omega^{(a)}$	$\xi^{(b)}$	$\chi_0^{(b)}$
$C-\alpha$	1.1 ± 0.1	2.0 ± 0.1	$(6 \pm 4)^\circ$	$(13 \pm 2)^\circ$	$(-33 \mp 2)^\circ$	$(-41 \mp 2)^\circ$
$N-\alpha$	0.8 ± 0.1	4.0 ± 0.2	$(6 \pm 4)^\circ$	$(13 \pm 2)^\circ$	$(-33 \mp 2)^\circ$	$(-41 \mp 2)^\circ$
$O-\alpha$	0.48 ± 0.05	4.0 ± 0.2	$(6 \pm 4)^\circ$	$(13 \pm 2)^\circ$	$(-33 \mp 2)^\circ$	$(-41 \mp 2)^\circ$

Coincidences $(10^{-2} sr^{-1})$	$C_{NE}^{(a)}$	$\lambda^{(a)}$	$h_0^{(a)}$	ϕ_R	$\phi_0^{(b)}$
$C-\alpha$	4.4 ± 0.4	2.5 ± 0.3	0.25 ± 0.03	$(30 \pm 3)^\circ$	$(57 \pm 3)^\circ$
$N-\alpha$	3.5 ± 0.4	2.3 ± 0.2	0.30 ± 0.04	$(38 \pm 3)^\circ$	$(57 \pm 3)^\circ$
$O-\alpha$	2.5 ± 0.3	2.4 ± 0.2	0.36 ± 0.05	$(40 \pm 3)^\circ$	$(57 \pm 3)^\circ$

The quantities obtained by fitting the experimental data by the evaporative formula (13) are labelled by (a). The quantities estimated from a simple inspection of the experimental angular correlation patterns by using the approximate expressions (21,22) are labelled by (b).

The parameter values for the three multiplicities are reported in Table I. Then, by assuming $(C_{NE}; \gamma; \Lambda_0)$ as free parameters, the complete experimental in-plane differential multiplicities (for $\alpha's$ and protons) were fitted after inserting the $(C_E; \gamma; \Lambda_0; \Omega; \xi; \chi_0)$ respective values previously determined, and finally the values for $(C_{NE}; \lambda; h_0)$ parameters were deduced.

When comparing the values of the C_E parameter reported in Table I at E_{lab} = 133 MeV to the value deduced in Table I of Ref. [11] with the same analysis at E_{lab} = 96 MeV, one can observe that the equilibrium components are approximately identical. In contrast, as the values of the C_{NE} parameter have increased by almost a factor 4, the nonequilibrium α-emission appears to follow an exponential increasing trend between 6 MeV/nucleon and 8.3 MeV/nucleon. However the target dependence (see Table II of Ref. [11] for the analysis of the data of the ^{48}Ti target at E_{lab} = 133 MeV for the comparison) of the nonequilibrium component is very weak. These results confirm the systematics previoulsy proposed by Ho *et al.* [6] (see Fig. 4 of Ref. [6]).

3.2.2 Proton emission in the ^{16}O + ^{56}Ni reaction

The same theoretical approach has been applied to the analysis of the PLF-proton angular correlations. Fig. 5 shows the calculations (solid lines for the NE component and dashed lines for the equilibrium component) of the in-plane differential multiplicities of $C-p$, $N-p$ and $O-p$ vs. the φ_p angle. From Table II it can be seen that, whereas the nonequilibrium components for protons are comparable to the that for *alpha* particles, the equilibrium components are large by at least a factor 2.

From the analysis of the fit parameters reported in Tables I and II, one easily infers that the spin direction is almost perpendicular to the reaction plane, as we supposed in the theoretical approach. As a matter of fact, the average value found

for the angle between the spin direction and the normal axis ($\Lambda_0 \leq 10^\circ$) confirms this hypothesis for all three coincidences. The non-equilibrium component consists of two bumps; the higher one is associated with the positive polarization, the lower with the negative one. The width of the peaks is related to the model parameter λ which represents the width of the ℓ-window mainly contributing to the decay process; such a value does not exceed $3\hbar$, thus confirming that we are dealing with a peripheral process. The last parameter obtained by the fit is ξ, which is related to the direction ϕ_0 of the momentum transferred to the projectile-target interaction; in the case of hard spheres, this direction would correspond to the recoil direction of the TLF (ϕ_R). As one can deduce from Tables I and II, the difference between these angles decreases for decreasing projectile-target mass transfer.

Table 2: **List of the parameters obtained in the analysis of the in-plane PLF-proton angular correlations arising from the ^{16}O(133 MeV) + ^{58}Ni reaction.**

Coincidences ($10^{-2} sr^{-1}$)	$C_E^{(a)}$	$\gamma^{(a)}$	$\Lambda_0^{(a)}$	$\Omega^{(a)}$	$\xi^{(b)}$	$\chi_0^{(b)}$
$C-p$	2.2 ± 0.2	0.5 ± 0.03	$(6 \pm 4)^\circ$	$(13 \pm 2)^\circ$	$(-35 \mp 2)^\circ$	$(-28 \mp 2)^\circ$
$N-p$	1.9 ± 0.2	1.3 ± 0.07	$(6 \pm 4)^\circ$	$(13 \pm 2)^\circ$	$(-39 \mp 2)^\circ$	$(-35 \mp 2)^\circ$
$O-p$	1.3 ± 0.1	2.0 ± 0.1	$(6 \pm 4)^\circ$	$(13 \pm 2)^\circ$	$(-37 \mp 2)^\circ$	$(-29 \mp 2)^\circ$

Coincidences ($10^{-2} sr^{-1}$)	$C_{NE}^{(a)}$	$\lambda^{(a)}$	$h_0^{(a)}$	ϕ_R	$\phi_0^{(b)}$
$C-\alpha$	4.0 ± 0.4	2.7 ± 0.3	0.29 ± 0.04	$(31 \pm 3)^\circ$	$(57 \pm 3)^\circ$
$N-\alpha$	2.8 ± 0.3	2.4 ± 0.2	0.14 ± 0.02	$(38 \pm 3)^\circ$	$(57 \pm 3)^\circ$
$O-\alpha$	3.0 ± 0.3	2.6 ± 0.3	0.16 ± 0.02	$(43 \pm 3)^\circ$	$(57 \pm 3)^\circ$

The quantities obtained by fitting the experimental data by the evaporative formula (13) are labelled by (a). The quantities estimated from a simple inspection of the experimental angular correlation patterns by using the approximate expressions (21,22) are labelled by (b).

In addition, one can obtain a rough estimate of the in-plane integrated sequential E and NE α-emissions for the processes considered here; in fact, in the case of $\vartheta = \pi/2$, we can get

$$\int_{-\pi}^{\pi} d\phi M(\phi) = M^E + M^{NE} \tag{21}$$

with

$$M^E \sim \pi C_E (1 - \exp(-\gamma)), \tag{22}$$

$$M^{NE} \sim C_{NE}(1 + h_0)/\lambda. \tag{23}$$

The values of $M^E + M^{NE}$, estimated within 30%, are listed in Table III.

Although NE processes contribute at the percentage level at low bombarding energy, they cannot be neglected at increasing bombarding energies.

As usual in our treatment, we can define a positive alignment parameter on a quantization axis perpendicular to the reaction plane as (omitting the explicit indication of ω_b)

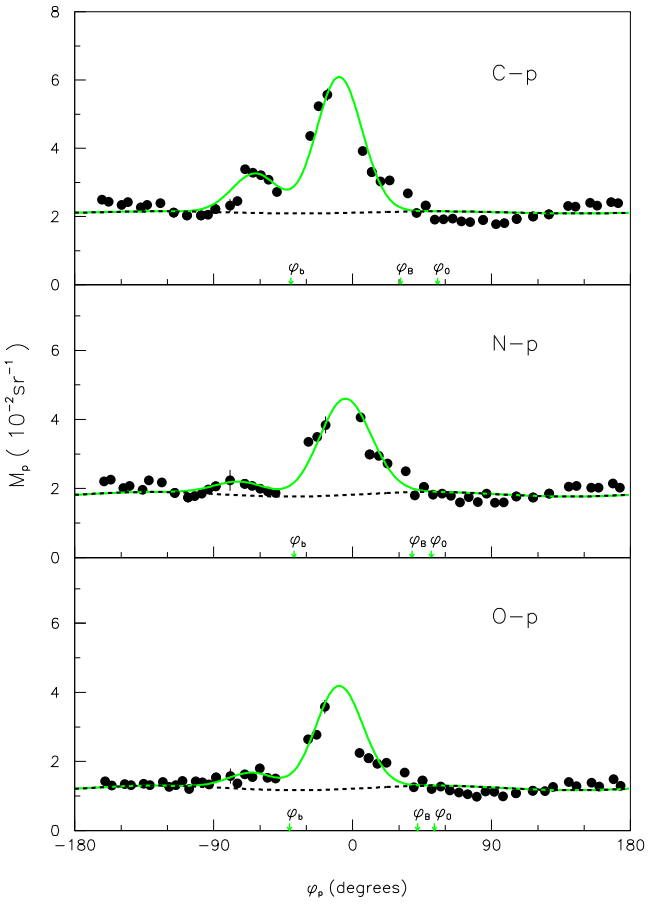

Figure 5: *Best-fit of the in-plane $C-p$, $N-p$ and $O-p$ differential multiplicity data, for the sequential process $^{16}O+^{58}Ni$ at E_{lab} = 133 MeV. The differential multiplicities, in $10^{-2}sr^{-1}$ units, are plotted vs. the in-plane proton-angle. The arrows indicate the directions of the PLF (b) and TLF (B) with respect to the incident beam in the laboratory system. The solid curves represent the total multiplicities, while the dashed curves represent the equilibrium component.*

Table 3: Values of rough approximations of M^E and M^{NE} for the PLF-α and PLF-p angular correlations from the $^{16}O(133\ \mathrm{MeV}) + {}^{58}Ni$ reaction.

Coincidences	$PLF-\alpha$		$PLF-proton$	
	M^E	M^{NE}	M^E	M^{NE}
$C-(light-particle)$	4.1	1.2	2.7	1.9
$N-(light-particle)$	2.8	1.1	4.3	1.3
$O-(light-particle)$	1.5	0.4	3.5	1.3

$$p_0 = \mid f_{ba}(m_0) \mid^2 / (\mid f_{ba}(m_0) \mid^2 + \mid f_{ba}(-m_0) \mid^2) = (1+h_0)^{-1},$$

Table 4: Values of p_0 parameters for the PLF-α and PLF-p angular correlations from the $^{16}O(133\ \mathrm{MeV}) + {}^{58}Ni$ reaction.

p_0 for Coincidences	C	N	O
α	0.80	0.77	0.74
p	0.78	0.88	0.86

whose values are reported in Table IV. The values of the polarization parameters for protons are roughly greater than those ones obtained for the α-emission. This means that the information about the polarization induced on the TLF's by the first step of the reaction is more important by studying the proton emission.

According to the Wilczynski model of DI reactions [31], which attributes the energy dissipation to frictional forces arising in the projectile-target contact region, up and down polarization can be related to positive and negative deflection function, respectively. Then, the observed positive polarization can be explained by assuming [30] that only one kind of *semiclassical trajectory*, i.e. the *far-side* one, predominantly contributes to the nonequilibrium component of the sequential emission.

An interesting feature of the reaction mechanism can be obtained by observing that [14] the half-angle between the two peaks, χ_0, can be related to the lifetime of the emitting nucleus [4] according to Eq. (18), where $\mathcal{I}$ is calculated as:

$$\mathcal{I} \approx \mathcal{I}_{rigid} \approx 0.0137 A^{5/3} \hbar^2.$$

Eq. (26), applied to our reaction whereby $\ell_0 \simeq 4\hbar$, gives

$$\tau_0 \simeq 5 \times 10^{-22} s \quad \text{for } \alpha, \text{ and}$$

$$\tau_0 \simeq 7 \times 10^{-22} s \quad \text{for protons}$$

as an estimate of the "decay time" after the formation of the B decaying nucleus. The results summarized in Table IV are consistent with the "decay times" deduced in Ref. Barna01 for the ^{16}O(96 MeV) + ^{58}Ni and ^{16}O(133 MeV) + ^{48}Ti reactions.

4 SUMMARY AND CONCLUDING REMARKS

The differential multiplicities obtained for both the α particles and the protons have been measured for the $^{16}O + {}^{58}Ni$ reaction at 8.3 MeV/nucleon using the ICARE charged-particle multidetector array [15, 16, 17] for energy-damped events. A newly developed theoretical semiclassical approach [11], assuming the hypothesis of a two-step sequential process, is successfully applied to analyse the measured angular correlations between α particles and protons detected in coincidence with the deep-inelastic projectile-like fragments more deeply and quantitatively.

From this analysis, one infers that the angular interval between the average transferred momentum in the $^{58}Ni(^{16}O, b)B$ reaction and the recoil nucleus B direction increases with the transferred mass from ^{16}O nucleus to ^{58}Ni nucleus. Many of the observed features of the sequential equilibrium emission and nonequilibrium emission are well reproduced for both the α particles and the protons by means of this simple semiclassical approach [11]. In particular, we have found for the first time that nonequilibrium proton emission exists significantly in the DI processes of the ^{16}O + ^{58}Ni reaction. Some information of the reaction mechanisms has been extracted, such as polarization phenomena (which are more sensitive for proton-emission than α-emission) or estimates of "decay times". By a comparions of the present analysis of the ^{16}O + ^{58}Ni reaction to previous one [11] of the ^{16}O + ^{44}Ti reaction, the target dependence of the nonequilibrium α-emission is found to be rather weak. The projetile dependence of both the nonequilibrium α- and proton-emissions have still to be investigated in a systematical manner. Therefore, this work may stimulate further experimental studies on different nuclear systems aimed at a deeper investigation of the timescales (lifetimes of the targetlike fragments and "decay times" of the formed dinucler systems) involved in DI collisions.

ACKNOWLEDGEMENTS

The authors wish to thank the staff of the VIVITRON for providing us with good ^{16}O stable beams, M.A. Saettel for preparing the targets, and J. Devin and C. Fuchs for the excellent support in carrying out these experiments. We wish also to thank L. Romano for a careful reading of the manuscript.

References

[1] W.U. Schröder and J.R. Huizenga, in *Treatise on Heavy-Ion Science*, edited by D.A. Bromley, Nuclear Sciences Vol. 2 (Plenum, New York, 1994).

[2] H. Ho, P. L. Gonthier, M. N. Namboodiri, J. B. Natowitz, L. Adler, S. Simon, K. Hagel, R. Terry, and A. Khodai, Phys. Lett. **B96**, 51 (1980).

[3] T. C. Awes, G. Poggi, C. K. Gelbke, B. B. Back, B. G. Glagola, H. Breuer, and V. E. Viola Jr., Phys. Rev. C **24**, 89 (1981).

[4] H. Ho, R. Albrecht, H. Damjantschitsch, F. J. Demond, W. Kühn, J. Slemmer, J. P. Wurm, D. Disdier, V. Rauch, F. Scheibling, and T. Dössing, Z. Phys. **A300**, 205 (1981).

[5] R. K. Bhowmik, E. C. Pollacco, J. B. A. England, G. C. Morrison, and N. E.Sanderson, Nucl. Phys. **A363**, 516 (1981).

[6] H. Ho, P. L. Gonthier, W. Kühn, A. Pfoh, L. Schad, R. Wolski, J. P. Wurm, J. C. Adloff, D. Disdier, A. Kamili, V. Rauch, G. Rudolf, F. Scheibling and A. Strazzeri, Phys. Rev. C **27**, 584 (1983).

[7] H. Ho, G. Y. Fan, P. L. Gonthier, W. Kühn, B. Lindl, A. Pfoh, L. Schad, R. Wolski, J. P. Wurm, J. C. Adloff, D. Disdier, V. Rauch, and F. Scheibling, Nucl. Phys. **A437**, 465 (1985).

[8] B. Lindl, A. Brucker, M. Bantel, H. Ho, R. Muffler, L. Schad, M. G. Trauth, and J. P. Wurm, Z. Phys. **A328**, 85 (1987).

[9] W. Terlau, M. Burgel, A. Budzanowski, H. Fuchs, H. Homeyer, G. Roschert, J. Uckert, and R. Vogel, Z. Phys. **A330**, 303 (1988).

[10] M. F. Vineyard, S. E. Atencio, J. F. Crum, G. P. Gilfoyle, B. G. Glagola, D. J. Henderson, D. G. Kovar, C. F. Maguire, J. F. Mateja, R. G. Ohl, F. W. Prosser, J. H. Rollinson, and R. S. Trotter, Phys. Rev. C **49**, 948 (1994).

[11] R. Barná, D. De Pasquale, A. Italiano, A. Trifiró, M. Trimarchi, A. Strazzeri, V. Rauch, D. Disdier, C. Beck, T. Bellot, R.M. Freeman, R. Nouicer, M. Rousseau, and O. Stezowski, Phys. Rev. C **64**, 054601 (2001).

[12] A. Strazzeri, Nuovo Cim. **A52**, 323 (1979).

[13] A. Strazzeri, Nuovo Cim. **A80**, 35 (1984).

[14] A. Italiano, A. Trifiró, G. Pisent and A. Strazzeri, Nuovo Cim. **A110**, 781 (1997).

[15] G. Bélier, Ph.D. thesis, Strasbourg University, Report **CRN-94-34** (1994) (unpublished).

[16] T. Bellot, Ph.D. thesis, Strasbourg University, Report **IReS-97-35** (1997) (unpublithed).

[17] M. Rousseau, Ph.D. thesis, Strasbourg University, Report **IReS 01-02** (2001) (unpublished).

[18] R. Barná, D. De Pasquale, A. Italiano, A. Trifiró, M. Trimarchi, V. Rauch, C. Beck, F. Haas, M. Rousseau, O. Stezowski, and A. Strazzeri, in *Proceedings of the IV Latin American Symposium on Nuclear Physics*, Mexico City, Mexico, September 24-28, 2001 (to be published in Heavy-Ion Science); Report **IReS-01-14** (2001).

[19] C. Bhattacharya, M. Rousseau, C. Beck, V. Rauch, R.M. Freeman, D. Mahboub, R. Nouicer, P. Papka, O. Stezowski, A. Hachem, E. Martin, A.K. Dummer, S.J. Sanders, and A. Szanto De Toledo, Phys. Rev. C **65**, 014611 (2002).

[20] M. Rousseau, C. Beck, C. Bhattacharya, V. Rauch, O. Dorvaux, K. Eddahbi, C. Enaux, R.M. Freeman, F. Haas, D. Mahboub, R. Nouicer, P. Papka, O. Stezowski, S. Szilner, A. Hachem, E. Martin, S.J. Sanders, A.K. Dummer, and A. Szanto De Toledo, Preprint **nucl-ex/0201021** and Report **IReS 02-01** (2002) (submitted to Phys. Rev. C).

[21] H. Feshbach, C. E. Porter and V. F. Weisskopf, Phys. Rev. **96**, 448 (1954).

[22] M. A. Preston, *Physics of the Nucleus* (Addison-Wesley, Reading, MA, 1963).

[23] W. Hauser and H. Feshbach, Phys. Rev. **87**, 366 (1952).

[24] F. L. Friedman and V. F. Weisskopf, *Niels Bohr and the Development of Physics* (McGraw-Hill, London, 1955).

[25] H. Eichner, H. Stehle and P. Heiss, Nucl. Phys. **A205**, 249 (1973).

[26] T. Ericson and V. Strutinsky, Nucl. Phys. **8**, 284 (1958).

[27] M. Lefort, in *Proceedings of the International School of Physics "Erico Fermi"*, Course LXII, Varenna, edited by H. Faraggi and R. A. Ricci (North-Holland, Amsterdam, 1976).

[28] N. K. Glendenning, *International Conference on Reactions between Complex Nuclei*, Nashville, 1974, Vol. 2, p. 137.

[29] V. M. Strutinsky, Sov. Phys. JETP **19**, 1401 (1964).

[30] P. D. Bond, Phys. Rev. C **22**, 1539 (1980); Phys. Rev. Lett. **40**, 501 (1978).

[31] J. Wilczynski, Phys. Lett. **47B**, 484 (1973).